Chemistry–A European Journal
Research Article
doi.org/10.1002/chem.202301273
Chemistry Europe
European Chemical Societies Publishing
www.chemeurj.org

Special Collection

σ,π-Conjugated Bis(germylene) Adducts with NHC and CAACs

Anna-Lena Thömmes,[a] Bernd Morgenstern,[b] Michael Zimmer,[a] Diego M. Andrada,[a] and David Scheschkewitz*[a]

Abstract: Heavier tetrylenes attract attention for their potential in synthesis, catalysis and small molecule activation. The coordination by *N*-heterocyclic carbenes (NHCs) and cyclic (alkyl)(amino)carbenes (CAACs) results in substantial structural and electronic differences although typically only one of these yields stable derivatives for one and the same tetrylene. We now report both NHC- and CAAC-coordination to a bridged bis(germylene) motif. The NHC-coordinated bis(germylene) exhibits pyramidal germanium centers with lone pairs of electrons, while with CAAC an unprecedented stable bis(germene) with two Ge=C bonds is isolated. Spectroscopic and crystallographic evidence as well as DFT calculations confirm the effects of σ,π-conjugation between the two germanium centers in both cases. The coordination of NHC is reversible as the reaction with BPh_3 liberates the transient bis(germylene) and thus provides an alternative low-temperature route towards polymers with Ge=Ge bonds.

Introduction

Heavier low-valent group 14 compounds with their exceptional electronic structures and versatile reactivity continue to be at the focus for their role in synthesis, catalysis and small molecule activation.[1] In particular, heavier carbene analogues (tetrylenes) and their dimers have been studied extensively during the past decades.[2] The kinetic stabilization of otherwise transient derivatives is achieved by bulky substituents, often complemented by the additional thermodynamic stability offered by intra- or intermolecular electron donors.[2b–e] *N*-Heterocyclic carbenes (NHCs) and cyclic (alkyl)(amino)carbenes (CAACs) have been employed as strong σ-donors in a variety of low-valent main group compounds.[3–9] The coordination of NHCs vs. CAACs often leads to drastic differences in (electronic) structure due to the stronger π-acceptor and σ-donor abilities of the latter. This has been evaluated experimentally and theoretically for group 13 and 15 with anionic borafluorenes by the Gilliard group,[10] the diborene carbene adducts by Engels et al.[11] or the carbene phosphinidene adducts by Bertrand et al.[12] In group 14, the considerably shorter Si–C_{CAAC} bond distances in the $(CAAC\cdot SiR)_2$ adducts (R=Cl, H, Me)[13] compared to the corresponding NHC adduct $(NHC\cdot SiCl)_2$[14] underpin these differences despite the pyramidal coordination environments of both adjacent tetrel(II) centers. In case of dihalosilylenes, predominantly NHC adducts have been reported.[15,16] The corresponding 1:1 adducts with CAAC apparently retain considerable electrophilicity leading to the addition of a second carbene equivalent as, for example, during the formation of Roesky's $(CAAC)_2\cdot SiCl_2$ diradical[17] or the addition of an NHC to the only isolated derivative, the equally pyramidal $CAAC\cdot SiI_2$.[18,19]

As concerns of germanium, after the groundbreaking isolation of the diiodogermylene-NHC adduct **I** by Arduengo et al. in 1993,[20] numerous pyramidal NHC adducts with germylenes have been reported.[21–27] The first diarylgermylene-NHC adduct **II** was obtained by Baines et al. in 2007 by cleavage of the corresponding digermene by an NHC.[28] All CAAC-adducts of halogermylenes exhibit a pyramidal structure comparable to the corresponding NHC adducts, irrespective of the nature of the halogen and despite the pronounced π-accepting ability of CAACs.[29,30] With the extremely electron-rich digermylenylgermene **III**[31] (Scheme 1), only one tetrylene-CAAC adduct with a genuine Ge=C double bond is known.

Neither NHC nor CAAC adducts of bridged bis(tetrylenes) with organic or inorganic linking units have been reported, presumably because known bis(tetrylenes) are without exception stabilized by internal donation of adjacent n-donor substituents at both tetrel(II) centers.[32–57] The thus reduced electron deficiency is obviously detrimental to formation of adducts with external donors. Recently, we reported the polymerization of the heavier acyclic diene **1** to give Ge=Ge containing polymer **2** via the postulated bis(germylene) **[3]** as

---

[a] A.-L. Thömmes, Dr. M. Zimmer, Dr. D. M. Andrada,
Prof. Dr. D. Scheschkewitz
Chair in General and Inorganic Chemistry
Saarland University
Campus Geb. C4 1, 66123 Saarbrücken (Germany)
E-mail: scheschkewitz@mx.uni-saarland.de
Homepage: http://www.uni-saarland.de/lehrstuhl/scheschkewitz.html

[b] Dr. B. Morgenstern
Inorganic Solid State Chemistry
Saarland University
Campus Geb. C4 1, 66123 Saarbrücken (Germany)

Supporting information for this article is available on the WWW under https://doi.org/10.1002/chem.202301273

Part of a Special Collection on the p-block elements.

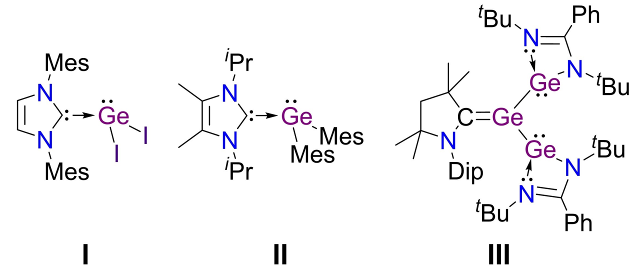

Scheme 1. Selected examples of germylene carbene adducts (Mes = 2,4,6-trimethylphenyl, Dip = 2,6-diisopropylphenyl).

key intermediate of a procedure dubbed as Heavier Acyclic Diene Metathesis (HADMET; Scheme 2).[58] Trapping of the monogermylene related to **[3]** by Et_3SiH suggested its pronounced electrophilicity at both germanium(II) centers. We therefore became curious about the effect of the σ,π-conjugated linking unit on the interaction of **[3]** with stable carbenes.

Results and Discussion

Indeed, the $GeTip_2$ moieties of **1** are easily substituted by NHC as well as by CAAC donors to afford the corresponding bis(carbene) adducts. As will be shown, the σ,π-conjugation between the germanium(II) centers is a main factor in determining the nature of the interaction of the carbene moieties with the germanium centers.

During the polymerization of the heavier acyclic diene precursor **1**, the dissociation of the $Ge{=}Ge$ bond is induced thermally by heating to 65 °C.[58] In order to prove the intermediacy of bis(silylgermylene) **[3]**, we repeated the reaction in the presence of Et_3SiH. The bridged bis(silylgermane) was indeed obtained as double Si–H insertion product along with the concomitantly formed silylgermane[58] (Scheme 3). Two ^{1}H NMR resonances in the characteristic range for Ge–*H* protons at 4.22 and 4.19 ppm indicate the formation of the diastereomeric mixture of the oxidative addition product. In the $^{29}Si/^{1}H$ HMBC NMR spectrum, cross peaks of the ^{1}H signals to the $^{29}Si\{^{1}H\}$ NMR signals of the Et_3Si (4.54, 5.51 ppm) and the Me_2Si moieties (−8.73, −9.08 ppm) confirm the connectivity.

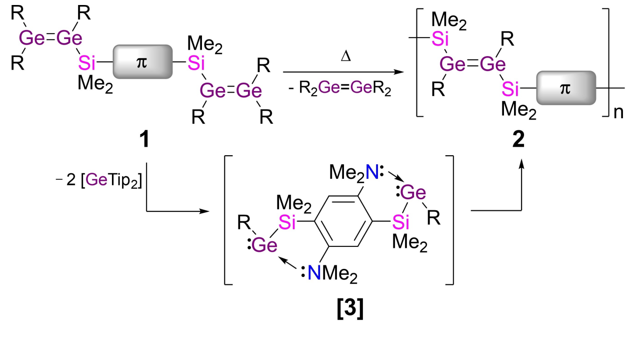

Scheme 2. Previously reported HADMET polymerization of **1** via transient bis(germylene) **[3]** (R=Tip = 2,4,6-triisopropylphenyl, π = *N,N,N′,N′*-tetramethyl-2,5-phenylenediamine).[58]

Baines et al. had shown that the dissociation of digermenes can also be initiated by addition of an NHC.[27,28] As a preliminary test, we therefore added four equivalents of Me_2IPr to the linker-separated tetragermadiene **1** at room temperature, which indeed resulted in the clean formation of two products in the 1:2 ratio required by the stoichiometry of the reaction. The bis(germylene)/Me_2IPr adduct **4** (Scheme 4) precipitates from the reaction mixture as a yellow solid in 63 % yield. The concomitantly formed, equally yellow NHC-$GeTip_2$ adduct was isolated from the concentrated mother liquor in 38 % yield by precipitation with pentane.

The presence of stereochemically active lone pairs at both germanium atoms in **4** is confirmed by the ^{1}H, $^{13}C\{^{1}H\}$ and $^{29}Si\{^{1}H\}$ NMR spectra, which each exhibit two similar sets of signals suggesting a 1:1 diastereomeric mixture. The $^{29}Si\{^{1}H\}$ signals of equal intensity at −11.07 and −11.19 ppm are in the range of σ,π-conjugated silyl groups (20.9 to −21.2 ppm).[59,60] The slight upfield shift compared to the parent tetragermadiene **1** (4.27 ppm)[58] and silyldigermenes and -germylenes in general (13.5 to −2.7 ppm)[27,58,61,62] is in line with a certain donation of

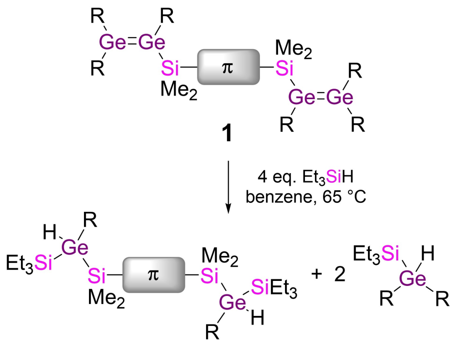

Scheme 3. Silane trapping of bis(germylene) **[3]** released from bis(digermene) **1** (R=Tip = 2,4,6-triisopropylphenyl, π = *N,N,N′,N′*-tetramethyl-2,5-phenylenediamine).

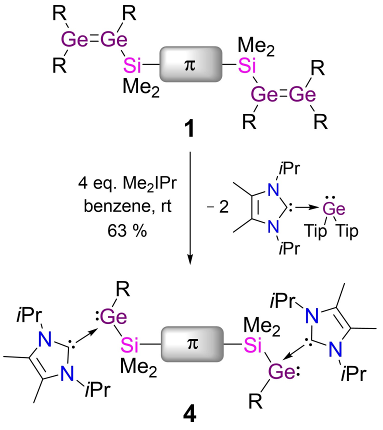

Scheme 4. Synthesis of NHC-stabilized germylene **4** (R=Tip = 2,4,6-triisopropylphenyl, π = *N,N,N′,N′*-tetramethyl-2,5-phenylenediamine).

the germanium-centered lone pairs of **4** to σ*-orbitals at the $SiMe_2$ bridge. The characteristic ^1H and $^{13}C\{^1H\}$ signals of the Me_2IPr methine groups (5.54 ppm) and the carbenic carbons (177.08, 177.00 ppm) confirm the coordination of Me_2IPr to the germanium centers.[19,20,23,27,28,63–67] The $GeTip_2/Me_2IPr$ adduct shows similar ^1H NMR septets at 5.64 and 5.34 ppm and a $^{13}C\{^1H\}$ resonance at 176.94 ppm for the coordinated Me_2IPr.

As crystallization attempts with bis(germylene) **4** remained unsuccessful, we also synthesized the mono(germylene)/NHC adduct **6** from digermene **5** in an analogous manner (Scheme 5). Similar characteristic resonances as for **4** were observed at 5.73 ppm in the ^1H, at 177.45 ppm in the $^{13}C\{^1H\}$ and at −11.49 ppm in the $^{29}Si\{^1H\}$ NMR spectrum. The ^1H and $^{13}C\{^1H\}$ spectra exhibit two sets of signals for the diastereotopic methyl groups at silicon, the Tip group and the NHC, respectively, in accordance with a pyramidal structure at germanium. Yellow single crystals of the NHC adduct **6** were grown from a pentane solution in 77% yield and analyzed by X-ray diffraction (Figure 1). The compound crystallized as a two component twin and was refined accordingly. There are two very similar molecules of **6** in the asymmetric unit, only one of which is referred to in the following: The relatively short Ge1–C16 bond of 2.070(6) Å is very close to those of the dimesitylgermylene-NHC complexes with IMe_4 (2.067(3) Å) and Me_2IPr (2.078(3) Å),[28] but far longer than typical Ge=C bond lengths (1.77–1.88 Å).[31,68,69] The Ge–Si distance (2.435(2) Å) is somewhat shorter than in an NHC-stabilized cyclic disilylgermylene (2.47, 2.48 Å)[43] and thus in line with partial interaction of the lone pair with the σ*-orbitals of the $SiMe_2$ bridge. Consequently, the Si–C bonds in **6** (1.89–1.90 Å) are slightly longer than in the disilylgermylenes (1.86–1.89 Å).[43] The substituents at the germanium center are arranged in a pyramidal manner (Σ°(Ge) = 311.7(6)°), which further supports the absence of significant Ge–C double bond character and instead confirms the existence of a stereochemically active lone pair at Ge as in similar compounds.[24] This is fully in line with the observation of diastereomers in case of the bis(NHC) adduct **4** in the multinuclear NMR spectra (see above).

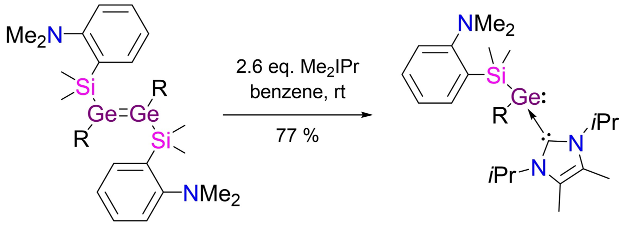

5 **6**

Scheme 5. Synthesis of mono(germylene)/NHC adduct **6** (R=Tip = 2,4,6-triisopropylphenyl).

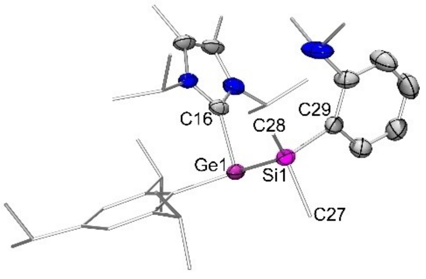

Figure 1. Molecular structure of NHC-germylene adduct **6** in the solid state (second molecule in asymmetric unit and hydrogen atoms omitted for clarity, thermal ellipsoids at 50%).[90] Selected bond lengths [Å] and angles [°]: Ge1–C16 2.070(6), Ge1–Si1 2.435(2), Si1–C27 1.891(6), Si1–C28 1.890(7), Si1–C29 1.900(7), Σ°(Ge1) 311.7(6).

The longest wavelength UV/Vis absorptions of bis(germylene) **4** are surprisingly intense: the broad band at $\lambda_{max} = 395$ nm shows an extinction coefficient of $\varepsilon = 10500\ L\,mol^{-1}\,cm^{-1}$, which is more than twice as large as that of mono(germylene) **6** ($\lambda_{max} = 395$ nm, $\varepsilon = 4000\ L\,mol^{-1}\,cm^{-1}$). Despite the absence of a noticeable red-shift, this intensity increase is even more pronounced than that of π-conjugated tetrasiladienes in comparison with the corresponding disilenes,[70–73] strongly suggesting an intramolecular charge transfer (ICT) process.

In order to shed further light on the electronic structure, we performed DFT calculations at the BP86/def2-SVP level of theory. The HOMO of NHC-germylene adduct **6** is best represented by a lone pair at Ge with dominant s-character and only minor p-orbital admixture ($s^{0.7}p^{0.3}$, Figure 2). The LUMO is mainly located at the NHCs and the anilinyl substituent (Figure 2). TD-DFT calculations at the PBE0/def2-TZVP level of theory indeed support the assignment of the longest wavelength absorption to the HOMO→LUMO excitation and thus an n→π* ICT transition from the germanium center to the surrounding ligands. The postulated σ,π-conjugation via the $SiMe_2$ linker is further supported by visual inspection of the HOMO of **6** (Figure 2), which clearly indicates mixing of the lone pair n-orbital at Ge with the σ*-orbital of the Ge–Si bond. For bis(germylene) **4**, HOMO and HOMO−1 likewise represent one of the lone pairs at the germanium atoms with partial mutual contribution (see Supporting Information). They differ in energy by 0.08 eV, in agreement with a resonance interaction of the two germylene moieties. The decrease of the HOMO–LUMO gaps from germylene **6** (2.40 eV) to bis(germylene) **4** (2.27 eV) is attributed to conjugative destabilization of the HOMO and stabilization of the LUMO (see Supporting Information for energy levels of bis(germylene) **4**), a well-known effect of increasing the conjugation path length of π-conjugated systems[74–76] as well as σ,π-conjugated compounds.[59]

Second order perturbation theory determines the interaction energy of the Ge lone pair (NBO 1) with one of the

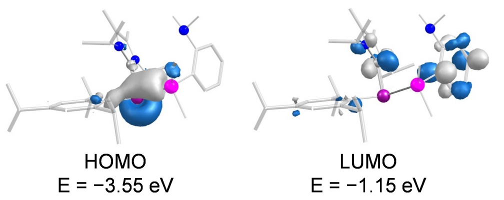

Figure 2. HOMO and LUMO of NHC-germylene **6** (contour value 0.052). Hydrogen atoms omitted for clarity.

antibonding σ*-orbitals of the $SiMe_2$ moiety (NBO 4) to 7.02 kcal mol^{-1} (Figure 3). The relatively low occupancy of NBO 1 of 1.81 e, together with the partially occupied (0.08 e) Si–C σ*-orbital (NBO 4) substantiate this further. Additionally, the Ge–Si bond (NBO 3) donates into NBO 5, another Si–C σ*-orbital, with an interaction energy of 2.04 kcal mol^{-1} and a reduced occupancy of 1.85 e. Consequently, the Ge–Si bond (NBO 3) is slightly polarized towards silicon (Figure 3) and the negative charge brought about by the NHC coordination is distributed across the aromatic substituents (confirmed by natural population analysis; see Supporting Information).

In line with the pronounced delocalization of the Ge-centered lone pair, neither NHC-bis(germylene) **4** nor $Tip_2Ge–Me_2IPr$ react as Lewis bases when BH_3–thf complex is added to a mixture of both. This is in sharp contrast to the reactivity of Baines' $Me_2IPr–GeMes_2$, which has been reported to form the corresponding BH_3-adduct.[28] While in the case of $GeTip_2$ the higher steric demand of the two Tip compared to two Mes groups is likely responsible, the bridged germylene **4** features the much less bulky silylene linker. The decreased nucleophilicity is thus arguably the result of substantial delocalization of the lone pair across the silicon center and the aromatic bridge.

Sterically encumbered, yet much more Lewis acidic BPh_3 on the other hand readily reacts with mono(germylene) **6** under NHC abstraction, giving rise to previously reported disilyldigermene **5**,[58] the dimerization product of the free germylene, along with $Me_2IPr–BPh_3$[77] (Scheme 6). Under the same conditions, bis(germylene) **4** provides an alternative and milder route towards poly(digermene) **2**:[58] Reaction of **4** with BPh_3 (Scheme 6) results in the immediate consumption of the starting material and precipitation of an insoluble yellow solid overnight, identified as polymer **2** by $^{13}C\{^1H\}$ and $^{29}Si\{^1H\}$ CP/MAS NMR spectroscopy.[59]

In light of the already pronounced delocalization of the Ge lone pairs in NHC-stabilized **4** into Si-centered σ*-orbitals, we became curious about the competing effect of a CAAC as strong π-acceptor. In contrast to Me_2IPr, cyclic (alkyl)(amino)carbene Me_4CAAC turned out to be inert towards tetragermadiene **1** at room temperature. Heating of **1** to 65 °C in the presence of an excess of Me_4CAAC, however, yields bis(germene) **7** and $Tip_2Ge{=}GeTip_2$ as the only detectable products (Scheme 7). The lower reactivity of Me_4CAAC compared to Me_2IPr is plausibly due to the higher steric congestion brought about by the Dip group at the nitrogen center. This assumption is underpinned by the fact that Dip-substituted 1,3-bis(2,6-diisopropylphenyl)imidazol-2-ylidene does not react at all with tetragermadiene **1**, even at elevated temperatures. Bis(germene) **7** is separated from $Tip_2Ge{=}GeTip_2$ by precipitation from thf as a yellow solid in 47 % yield. Its very low solubility in all common organic solvents prevents the characterization by multinuclear NMR in solution. The $^{29}Si\{^1H\}$ CP/MAS NMR, however, exhibits only one singlet at −5.77 ppm, upfield shifted compared to the solution resonance found for the precursor, digermene **1** (4.29 ppm).[77] In the $^{13}C\{^1H\}$ CP/MAS spectrum the carbene carbon peak is found at 194.3 ppm, considerably upfield shifted compared to the solution $^{13}C\{^1H\}$ NMR resonances of free Me_4CAAC (313.6 ppm)[78] and of the CAAC-germene **III** reported by Roesky et al. (219.4 ppm).[31]

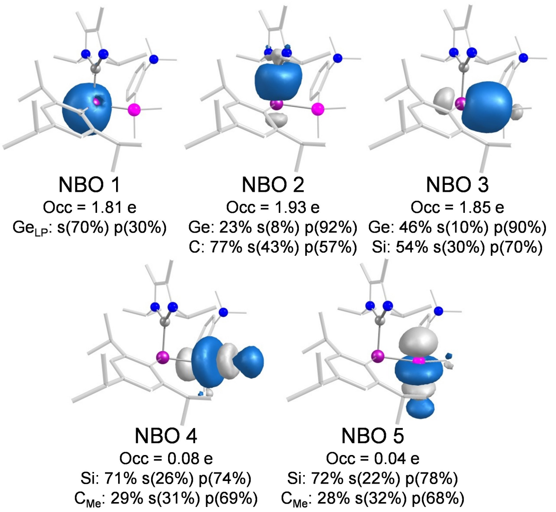

Figure 3. Selected NBOs of NHC-germylene **6** (contour value 0.043). Hydrogen atoms omitted for clarity.

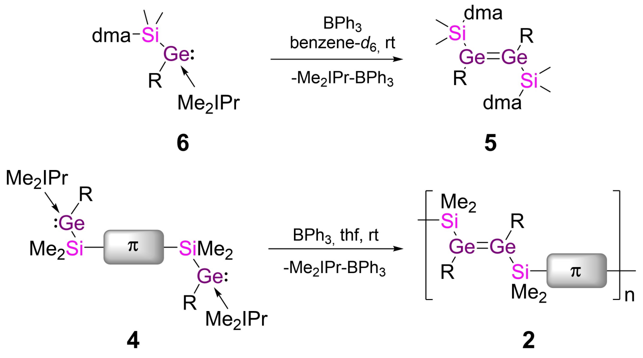

Scheme 6. NHC abstraction with BPh_3 (R=Tip = 2,4,6-triisopropylphenyl, dma = 2-*N*,*N*-dimethylanilinyl, π = *N*,*N*,*N'*,*N'*-tetramethyl-2,5-phenylenediamine).

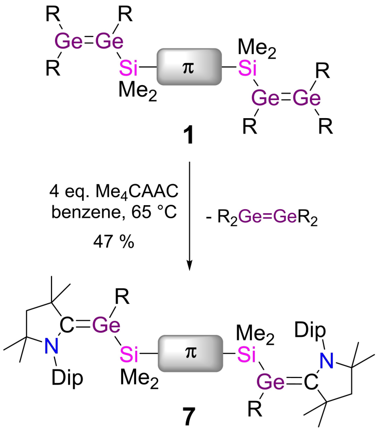

Scheme 7. Synthesis of $(Me_4CAAC)_2$-bis(germene) **7** (R=Tip = 2,4,6-triisopropylphenyl, π = *N*,*N*,*N'*,*N'*-tetramethyl-2,5-phenylenediamine).

Yellow crystals suitable for X-ray diffraction were directly obtained from a benzene solution of the reaction mixture. The molecular structure in the solid state shows the presence of the *Z*,*Z*-isomer of **7** (Figure 4).

The Ge–C distance of 1.825(2) Å is in the range of known Ge–C double bonds (1.77–1.88 Å).[31,68,69] In fact, it fits particularly well to the Ge–C distances of the conjugated acetylene bridged bis(germenes) reported by Weidenbruch (1.819, 1.819 Å).[79,80] With a sum of the angles of $\Sigma^{\circ}(\mathrm{Ge})=359.7(2)^{\circ}$ and $\Sigma^{\circ}(\mathrm{C})=359.6(5)^{\circ}$ there is only a slight deviation from planarity as also shown by the rather small *trans*-bent angles of $\Theta(\mathrm{Ge})=5.05(7)^{\circ}$ and $\Theta(\mathrm{C})=5.7(1)^{\circ}$, thus confirming the existence of a $\sigma+\pi$ double bond between Ge and C. In addition, the substituents are only slightly twisted ($\tau=5.8(1)^{\circ}$), comparable with other nearly planar germenes ($\tau=3.6^{\circ}$,[31] 5.9°,[81] 4°[82]). Noticeably, the Ge–C bond in **7** is not coplanar to the phenylene linker, but rather exhibits a pronounced dihedral angle of C8–Ge1–Si1–C3 = 78.03(9)°. This geometry allows for an optimal interaction of the π-bond with the antibonding σ*-orbitals of the $\mathrm{SiMe_2}$ group. Indeed, the Si–C bonds (1.87–1.90 Å) are slightly longer than in trimethylsilylalkyl and -aryl compounds (1.85–1.89 Å)[83–85] while the Ge1–Si1 distance (2.3699(9) Å) is considerably shorter than in tetragermadiene **1** (2.4007(7) Å).[58]

In the UV/Vis spectrum of bis(germene) **7** a broad absorption band is observed at $\lambda_{\mathrm{max}}=404$ nm, in between the longest absorption wavelengths of the disilylgermene of Haas et al. (368 nm),[69] transient germenes (262 to 325 nm)[86–88] and Weidenbruch's purely π-conjugated bis(germenes) (500–595 nm).[79,80] The extinction coefficient of bis(germene) **7** ($\varepsilon(404\ \mathrm{nm})=34000\ \mathrm{L\,mol^{-1}\,cm^{-1}}$) is almost twice as large as for tetragermadiene **1** ($\varepsilon(426\ \mathrm{nm})=17600\ \mathrm{L\,mol^{-1}\,cm^{-1}}$)[58] and even four times larger than for an acetylene linked π-conjugated bis(germene) ($\varepsilon(500\ \mathrm{nm})=8000\ \mathrm{L\,mol^{-1}\,cm^{-1}}$).[80] These properties are in accordance with the typical large absorption cross-section of strongly conjugated systems and suggest the relevance of σ,π-conjugation in this system. The experimental results are further underpinned by DFT computations at the BP86/def2-SVP level of theory. The experimentally found *Z*,*Z*-isomer is more stable than the *E*,*Z* isomer and the *E*,*E* isomer by 2.05 $\mathrm{kcal\,mol^{-1}}$ and 6.61 $\mathrm{kcal\,mol^{-1}}$, respectively, and was therefore used for further calculations. TD-DFT (BP86/def2TZVPP) identifies three bands at 437, 427 and 422 nm as due to the HOMO→LUMO + 1 and HOMO−1→LUMO + 2 transitions. Transitions from HOMO/HOMO−1 to the π*-orbital of the *para*-phenylene linker (LUMO + 3) also contribute significantly to these bands. Accordingly, HOMO and HOMO−1, representing the π-orbitals of the C=Ge double bonds, show considerable contribution of the σ*-orbital of the silyl linker as judged from visual inspection (Figure 5). They are not degenerate but separated by 0.08 eV. An identical separation is found between LUMO + 1 and LUMO + 2, the corresponding orbitals of π*-symmetry. The LUMO consists mainly of the π*-orbital of the *para*-phenylene linker and visibly shows admixture of the σ*(Si)-orbital. The energy gaps between HOMO−1 and LUMO + 1 and HOMO and LUMO + 2, each amount to only 2.10 eV. The occupied π-orbitals of the phenylene linker, HOMO−12 and HOMO−13 display a *para*-quinoid appearance including the $\mathrm{SiMe_2}$ groups (Figure 5). For example, the frontier orbitals of the *para*-phenylenediamine radical cation show a similar pattern with respect to the amino groups as part of the π-system.[89]

NBO analysis was performed on mono(germene) **8** as a model compound for comparison with the mono(germylene)/NHC adduct **6**. The optimized structure of **8** exhibits considerable deviation from planarity at the germanium center ($\Sigma^{\circ}(\mathrm{Ge})=350.9^{\circ}$), in stark contrast to the bis(germene) **7** ($\Sigma^{\circ}(\mathrm{Ge})=359.6^{\circ}$). Consequently, the Ge=C double bond is substantially stabilized electronically via the $\mathrm{SiMe_2}$-phenylene bridge, confirming the presence of conjugative interaction. Despite the slight pyramidalization at the germanium center,

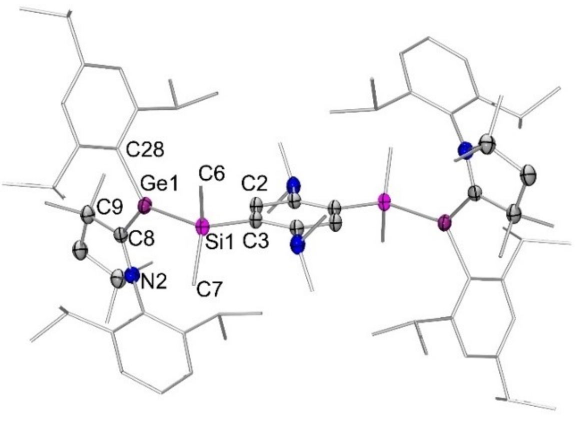

Figure 4. Molecular structure of bis(germene) **7** in the solid state (H atoms, co-crystallized benzene and disordered atoms omitted for clarity, thermal ellipsoids at 50%).[90] Selected bond lengths [Å] and angles [°]: Ge1–C8 1.825(2), Ge1–Si1 2.3699(9), Si1–C3 1.898(2), Si1–C6 1.879(3), Si1–C7 1.870(3), Σ°(Ge1) 359.7(2), Σ°(C8) 359.6(5), Θ(Ge1) 5.05(7), Θ(C8) 5.7(1), τ 5.8(1), Ge1–Si1–C3–C2 1.5(1), C8-Ge1–Si1–C3 78.03(9).

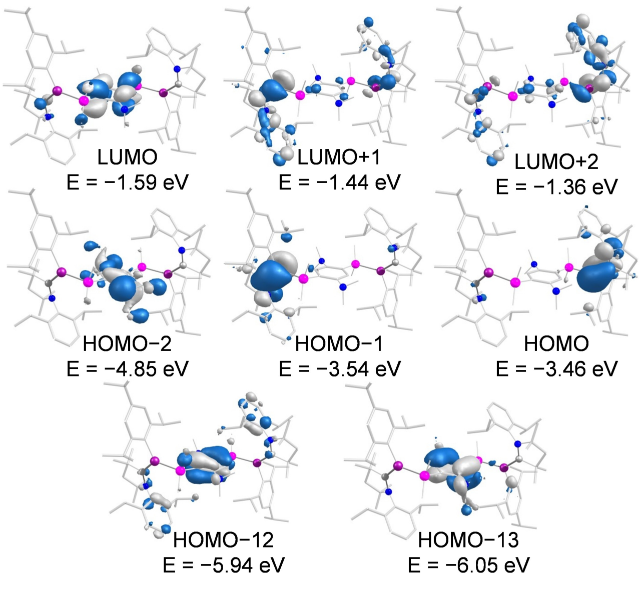

Figure 5. Selected frontier orbitals of bis(germene) **7** (contour value 0.036). Hydrogen atoms omitted for clarity.

the NBOs still confirm significant double bond character between Ge and C in mono(germene) **8** (NBO 1 and NBO 2; Figure 6) with a Wiberg bond index of 1.35.

The σ,π-conjugation in **7** gains further support from the NBO analysis of model compound **8**, which quantifies the interaction of the Ge–C π-bond (NBO 2, Figure 6) and the σ*-orbital of the Si–C_{dma} bond (NBO 4) to 3.43 kcal mol^{-1} (Figure 6). Notably, NBO 2 shows a slightly higher occupation of 1.85 e compared to 1.81 e of the Ge lone pair in the corresponding germylene-NHC adduct **6**. Owing to distinct donation, the σ* of the Si–C_{dma} bond (NBO 4) is occupied by 0.08 e. In line with the somewhat decreased delocalization in the CAAC adduct **8**, the Ge–Si σ-bond is slightly polarized towards germanium (NBO 3; Figure 6), in contrast to the NHC adduct **6** (NBO 3; Figure 3).

Consistent with distinct backdonation towards the carbene, monogermene **8** features a negative charge of −0.33 e at the CAAC substituent (see Supporting Information),[31] in stark contrast to the monogermylene/NHC adduct **6** with a positively charged NHC ligand (+0.32 e). Thus, unlike the case of the corresponding NHC adduct, the pronounced π-accepting ability of the CAAC enables the formation of Ge=C double bonds. The σ,π-conjugation across the silylphenylene linker provides the required electronic stabilization although to a lesser extent than in the bis(germylene)/NHC adduct **4**, presumably due to the stronger and hence more localized binding of the CAAC moiety.

In order to provide experimental evidence for the stronger bonds of the CAAC to the germylene fragments in comparison with those of the NHCs, NHC stabilized bis(germylene) **4** was treated with an excess of Me_4CAAC. Indeed, the reaction readily occurred even at room temperature to give bis(germene) **7** (Scheme 8). The much lower temperature and hence milder conditions compared to the reaction of **1** with CAAC, resulted in an increased yield of 57% (49% from **1**, Scheme 7).

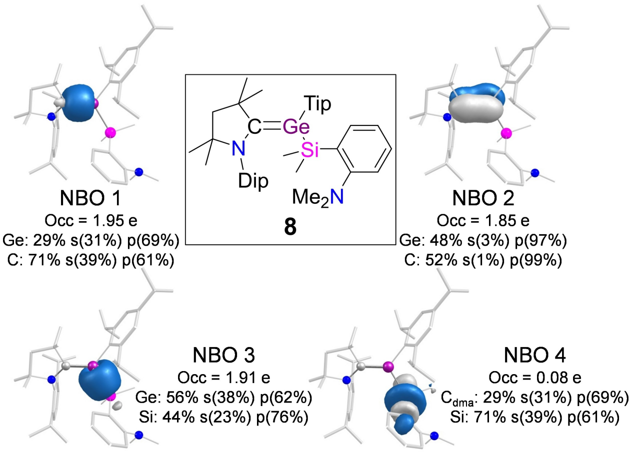

Figure 6. Structure of model germene **8** and selected NBOs (contour value 0.052). Hydrogen atoms omitted for clarity.

Conclusion

In conclusion, exchange of the $GeTip_2$ moiety in a bridged bis(digermene) provides the first NHC- and CAAC-stabilized bis(germylenes). While the Me_2IPr-germylene adduct exhibits pyramidal structures with a lone pair and a vacant p-orbital at the germanium centers, with Me_4CAAC the first example of a CAAC-based bis(germene) – featuring Ge=C double bonds – is formed. This is in stark contrast to most other known CAAC/germylene adducts which, despite the pronounced π-accepting ability of CAACs, have pyramidal structures.[29,30] The stronger bond between the germylene moiety and Me_4CAAC in comparison to Me_2IPr is demonstrated by the facile exchange reaction at room temperature. In both cases, for the NHC and the CAAC adducts with the bis(germylene), significant interaction between the unsaturated germanium centers through σ,π-conjugation across the linking unit is confirmed by crystallographic, spectroscopic and computational evidence. The hence decreased nucleophilicity of the lone pair prevents the reaction with BH_3-thf even for the NHC adduct. With the bulkier BPh_3, on the other hand, NHC abstraction is readily achieved, offering an alternative route to the recently reported polymer with Ge=Ge double bonds.[58] In addition, the generation of the transient bis(germylene) under mild conditions promises the wide application of such species in small molecule activation and catalysis.

Experimental Section

General considerations

All manipulations were carried out under a protective atmosphere of argon applying standard Schlenk or glovebox techniques. The glassware was pre-dried in oven at 125 °C and heated in vacuo prior to use. Solvents were dried and degassed by reflux over sodium/benzophenone under argon (thf, benzene) or taken from a solvent purification system (Innovative technology PureSolv MD7; diethylether, hexane, pentane). C_6D_6 and thf-d_8 were dried over potassium mirror and distilled under argon prior to use. Me_4CAAC,[91] Me_2IPr,[92] 1,3-bis(2,6-diisopropylphenyl)imidazol-2-

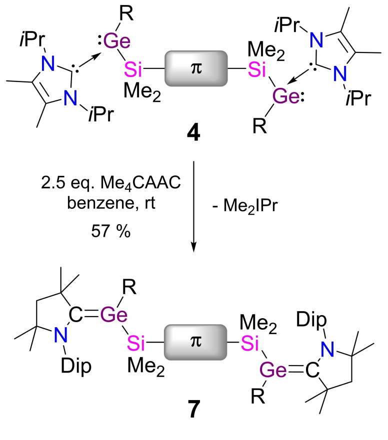

Scheme 8. Exchange reaction of NHC-bis(germylene) **4** with Me_4CAAC yielding the bis(germylene)/CAAC adduct **7**.

ylidene[93] and digermenes **1** and **5**[58] were prepared according to the published procedures. All other chemicals were obtained commercially and used as received. The NMR spectra were recorded on a Bruker Avance III HD 400 spectrometer (^{1}H: 400.13 MHz, ^{13}C: 100.61 MHz, ^{29}Si: 79.49) or on a Bruker Avance III HD 300 at 300 K (^{1}H: 300.13 MHz, ^{13}C: 75.56 MHz, ^{29}Si: 59.6 MHz). The ^{1}H and ^{13}C {^{1}H} NMR spectra were referenced to the residual proton and natural abundance ^{13}C resonances of the deuterated solvent and chemical shifts were reported relative to $SiMe_4$ (C_6D_6: $\delta^1H = 7.16$ ppm and $\delta^{13}C = 128.06$ ppm, thf-d_8: $\delta^1H = 1.78$, 3.58 ppm and $\delta^{13}C = 67.21$, 25.31 ppm).[94] The ^{29}Si NMR chemical shifts were referenced to external $SiMe_4$. The following abbreviations were used for the multiplicities: s – singlet, d – doublet, t – triplet, sept – septet, m – multiplet, brs – broad singlet. Solid state CP/MAS NMR spectra were recorded on a Bruker Avance III 400 WB at 13 kHz (^{13}C {^{1}H}: 100.61 MHz, ^{29}Si{^{1}H: 79.49 MHz). UV/Vis spectra were recorded on a Shimdazu UV-2600 spectrometer in quartz cells with a path length of 0.1 cm. Melting points were determined under argon in sealed NMR tubes and are uncorrected. The molten samples were examined by NMR spectroscopy to confirm whether decomposition had occurred upon melting. Elemental analyses were performed in triplicate for each sample using Leco CHN900 analyzer and mean values are given below for each compound. Crystallographic data was collected using a Bruker D8 Venture diffractometer with a microfocus sealed tube and a Photon II detector. Monochromated $Mo_{K\alpha}$ radiation ($\lambda = 0.71073$) was used. Data were collected at 133(2) K and corrected for absorption effects using the multi-scan method. The structure was solved by direct methods using SHELXT[95] and was refined by full matrix least squares calculations on F2 (SHELXL2018)[96] in the graphical user interface Shelxle.[97]

Synthesis of bis(germylene)/Me$_2$IPr adduct 4: Bis(digermene) **1** (1.5 g, 803 μmol) and Me_2IPr (579 mg, 3.21 mmol) are dissolved in 18.5 mL of benzene. Stirring for eight hours at room temperature is followed by filtration. Washing of the yellow solid with 2 mL of benzene yields bis(germylene)/Me_2IPr adduct **4** (624 mg, 63 %).* All volatiles are removed from the mother liquor in vacuo and the residue is dissolved in pentane. The yellow crystalline solid formed from this solution is separated by filtration and dried in vacuo to give $Tip_2Ge\cdot Me_2IPr$ (402 mg, 38 %).

* contains 0.6 wt.% of free Me_2IPr

NMR data of bis(germylene)/Me_2IPr adduct **4**:

^{1}H NMR (400.13 MHz, thf-d_8, 300 K, TMS): $\delta = 7.12$, 7.06 (each s, overall 2H, Ph*H*), 6.79 (s, 4H, Tip*H*), 5.54 (brs, 4H, C*H*(CH_3)$_2$ of Me_2IPr), 3.88 (brs, 4H, C*H*(CH_3)$_2$ of Tip), 2.73 (sept, 2H, C*H*(CH_3)$_2$ of Tip), 2.47 (s, 12H, N(C*H*$_3$)$_2$), 2.17 (s, 12H, Me_2IPr–CC*H*$_3$), 1.29 (d, 12H, CH(C*H*$_3$)$_2$ of Me_2IPr), 1.17 (d, 12H, CH(C*H*$_3$)$_2$ of Me_2IPr), 1.03 (d, 12H, CH(C*H*$_3$)$_2$ of Tip), 0.90 (d, 12H, CH(C*H*$_3$)$_2$ of Tip), 0.78, 0.76 (each d, overall 12H, CH(C*H*$_3$)$_2$ of Tip), 0.53, 0.52 (d, s, overall 12H, Si(C*H*$_3$)$_2$) ppm. **^{13}C {^{1}H} NMR** (100.61 MHz, thf-d_8, 300 K, TMS): $\delta = 177.08$, 177.00 (Me_2IPr–*C*), 155.93 (Ph*C*). 154.51, 151.67, 146.13, 142.49 (Tip*C*), 129.02, 128.85 (Me_2IPr–*C*CH_3), 126.75, 126.73 (Ph*C*), 120.72 (Tip*C*), 53.88 (*C*H(CH_3)$_2$ of Me_2IPr), 47.40 (N(*C*H$_3$)$_2$), 34.94 (*C*H(CH_3)$_2$ of Tip), 24.56, 24.47, 21.58, 21.55, (CH(*C*H$_3$)$_2$ of Tip), 20.58, 20.52 (CH(*C*H$_3$)$_2$ of Me_2IPr), 10.19 (Me_2IPr–C*C*H$_3$), 4.58, 4.48, 3.68, 3.55 (Si(*C*H$_3$)$_2$) ppm. **^{29}Si{^{1}H} NMR** (79.49 MHz, thf-d_8, 300 K, TMS): $\delta = -11.08$, -11.21 ppm. **UV/Vis** (*n*-hexane/thf = 80/20): $\lambda_{max} = 332$ nm ($\varepsilon = 15500\ L\,mol^{-1}\,cm^{-1}$), 395 nm ($\varepsilon = 10500\ L\,mol^{-1}\,cm^{-1}$). **Elemental analysis**: Calcd. for ($C_{66}H_{112}Ge_2N_6Si_2$): C, 66.55; H, 9.48; N, 7.06. Found: C, 66.94; H, 8.76; N, 6.55. **Mp.**: 162 °C (decomposition).

NMR data of $Tip_2Ge\cdot Me_2IPr$:

^{1}H NMR (400.13 MHz, thf-d_8, 300 K, TMS): $\delta = 7.22$ (s, 1H, Tip*H*), 7.17 (s, 1H, Tip*H*, overlapping with residual protons from C_6D_6), 5.64 (sept, 1H, C*H*(CH_3)$_2$ of Me_2IPr), 5.34 (sept, 1H, C*H*(CH_3)$_2$ of Me_2IPr), 4.59 (sept, 1H, C*H*(CH_3)$_2$ of Tip), 4.10 (sept, 1H, C*H*(CH_3)$_2$ of Tip), 4.00 (sept, 1H, C*H*(CH_3)$_2$ of Tip), 3.59 to 3.47 (m, 1H, C*H*(CH_3)$_2$ of Tip), 2.89 (sept, 2H, C*H*(CH_3)$_2$ of Tip), 1.76 (dd, 6H, CH(C*H*$_3$)$_2$ of Tip), 1.56 (d, 6H, CH(C*H*$_3$)$_2$ of Me_2IPr), 1.48, 1.45 (each d, overall 6H, CH(C*H*$_3$)$_2$ of Tip), 1.34 to 1.30 (m, 18H, CH(C*H*$_3$)$_2$ of Me_2IPr and Tip), 1.25 to 1.20 (m, 9H, CH(C*H*$_3$)$_2$ of Tip)m 1.15 (d, 3H, CH(C*H*$_3$)$_2$ of Tip), 1.02 (d, 6H, CH(C*H*$_3$)$_2$ of Tip) ppm. **^{13}C{^{1}H} NMR** (100.61 MHz, thf-d_8, 300 K, TMS): $\delta = 176.94$ (Me_2IPr–*C*), 156.76, 156.18, 155.78, 153.81, 151.20, 149.85, 147.44, 146.23 (Tip*C*), 128.18, 127.94 (*C*CH3 of Me_2IPr), 126.22, 125.30, 121.39 (Tip*C*), 120.84 (*C*CH$_3$of Me_2IPr), 120.51 (Tip*C*), 53.01, 52.05 (*C*H(CH_3)$_2$ of Me_2IPr), 37.70, 35.47, 34.76, 33.76, 33.42 (*C*H(CH_3)$_2$ of Tip), 26.61, 26.54, 25.99, 25.81, 25.45, 25.30, 24.70 to 24.47, 24.17, 23.97 (CH(*C*H$_3$)$_2$ of Tip), 21.61, 20.86, 20.77, 20.22 (CH(*C*H$_3$)$_2$ of Me_2IPr), 10.24, 10.08 (C*C*H$_3$ of Me_2IPr) ppm. **UV/Vis** (*n*-hexane): $\lambda_{max} = 313$ ($\varepsilon = 4700\ L\,mol^{-1}\,cm^{-1}$), 361 ($\varepsilon = 5900\ L\,mol^{-1}\,cm^{-1}$), 407 ($\varepsilon = 5400\ L\,mol^{-1}\,cm^{-1}$). **Elemental analysis**: Calcd. for ($C_{41}H_{66}GeN_2$): C, 74.66; H, 10.09; N, 4.25. Found: C, 72.50; H, 9.25; N, 4.30. **Mp.**: 136 °C (partial formation of $Tip_2Ge{=}GeTip_2$).

Synthesis of germylene/Me$_2$IPr adduct 6: Digermene **5** (420 mg, 411 μmol) and Me_2IPr (193 mg, 1.07 mmol) are dissolved in 9 mL of benzene. The resulting yellow solution is stirred at room temperature for overnight. After addition of another 9 mL of benzene, the reaction mixture is filtered. All volatile parts are removed in vacuo and the resulting red oil is dissolved in pentane. Yellow crystals of **6** are obtained from this solution at room temperature (211 mg, 77 %).*

* contains 5 wt.% of free Me_2IPr

^{1}H NMR (400.13 MHz, C_6D_6, 300 K, TMS): $\delta = 7.99$ (dd, 1H, Me_2N–Ph*H*) 7.27 to 7.20 (ddd, 1H, Me_2N–Ph*H*), 7.11 (s, 2H, Tip*H*), 7.09–7.05 (m, 2H, Me_2N–Ph*H*), 5.74 (sept, 2H, C*H*(CH_3)$_2$ of Me_2IPr), 4.24 (sept, 2H, C*H*(CH_3)$_2$ of Tip), 2.90 (sept, 1H, C*H*(CH_3)$_2$ of Tip), 2.63 (s, 6H, N(C*H*$_3$)$_2$), 1.56 (s, 6H, NHC–C*H*$_3$), 1.33, 1.33, 1.31 (each d, overall 12H, CH(C*H*$_3$)$_2$ of Me_2IPr), 1.13 (d, 6H, CH(C*H*$_3$)$_2$ of Tip), 1.04 (d, 6H, CH(C*H*$_3$)$_2$ of Tip), 0.97, 0.90 (each s, overall 6H, Si(C*H*$_3$)$_2$), 0.80 (d, 6H, CH(C*H*$_3$)$_2$ of Tip) ppm. **^{13}C{^{1}H} NMR** (100.61 MHz, C_6D_6, 300 K, TMS): $\delta = 177.45$ (Me_2IPr–*C*), 161.27 (Ph*C*), 154.72, 150.83, 146.45, 142.91 (Tip*C*), 137.82, 136.03 (Ph*C*), 128.96 (Me_2IPr–*C*CH$_3$), 125.81, 124.05 (Ph*C*), 120.92 (Tip*C*), 53.34 (*C*H(CH_3)$_2$ of Me_2IPr), 47.36 (N(*C*H$_3$)$_2$), 36.67, 34.72 (*C*H(CH_3)$_2$ of Tip), 25.63, 25.17 (CH(*C*H$_3$)$_2$ of Tip), 21.41, 20.57 (CH(*C*H$_3$)$_2$ of Me_2IPr), 9.99 (Me_2IPr–C*C*H$_3$), 4.45, 4.06 (Si(*C*H$_3$)$_2$) ppm. **^{29}Si{^{1}H} NMR** (79.49 MHz, C_6D_6, 300 K, TMS): $\delta = -11.49$ ppm. **UV/Vis** (*n*-hexane/thf = 80/20): $\lambda_{max} = 329$ nm ($\varepsilon = 6000\ L\,mol^{-1}\,cm^{-1}$), 395 nm ($\varepsilon = 4000\ L\,mol^{-1}\,cm^{-1}$). **Elemental analysis**: Calcd. for ($C_{36}H_{59}GeN_3Si$): C, 68.14; H, 9.37; N, 6.62. Found: C, 67.96; H, 9.04; N, 6.67. **Mp.**: 135 °C.

Synthesis of bis(germylene)/Me$_4$CAAC adduct 7: Bis(digermene) **1** (1.05 g, 565 μmol) and Me_4CAAC (740 mg, 2.59 mmol) are dissolved in 10 mL of benzene. The red solution is heated to 65 °C overnight. The solvent is distilled off in vacuo and the residue is stirred in 6 mL of thf at 65 °C for a few minutes. The soluble parts are filtered off and the residue is washed three times with overall 12 mL of thf. Bis(germene) **7** is obtained as a yellow solid, which is dried in vacuo (368 mg, 47 %). Single crystals of **7** are obtained directly from the reaction mixture in C_6D_6.

^{13}C{^{1}H} CP/MAS NMR (100.61 MHz, 300 K, 13 kHz, TMS): $\delta = 194.31$ (Me_4CAAC–*C*), 157.13, 154.17, 148.62, 142.93, 141.52, 139.42, 133.66, 126.05, 123.84, 122.27, 119.60 (Ph*C*, Tip*C* and Dip*C*), 66.32 (N(*C*H$_3$)$_2$), 58.44 (C_q of Me_4CAAC), 49.82 (*C*H(CH_3)$_2$ of Tip and Dip), 47.20 (C_q of Me_4CAAC), 37.75, 35.26, 34.18, 33.09 (*C*H(CH_3)$_2$ of Tip and Dip), 25.51 (CH_3 of Tip and Dip), 0.81 (Si(CH_3)$_2$). **^{29}Si{^{1}H} CP/MAS NMR** (79.49 MHz, 300 K, 13 kHz, TMS): $\delta = -5.77$ ppm. **UV/Vis** (*n*-hexane/thf = 80/20): $\lambda_{max} = 404$ nm ($\varepsilon = 34000\ L\,mol^{-1}\,cm^{-1}$). **Elemental anal-**

ysis: Calcd. for ($C_{84}H_{134}Ge_2N_4Si_2$): C, 71.99; H, 9.64, N, 4.00. Found: C, 71.68; H, 9.22; N, 4.26. **Mp.:** 220 °C (decomposition).

Supporting Information

Detailed experimental, analytical and computational data are contained in the Supporting Information. Additional references cited within the Supporting Information.[98–105]

Supplementary crystallographic data see Ref. [90].

Acknowledgements

We thank the Fonds der Chemischen Industrie for a Kekulé fellowship for A.-L.T. We also acknowledge the instrumentation facilities provided by the service center for X-ray analysis established with the financial support from Saarland University and German Research Foundation (INST 256/506-1). Open Access funding enabled and organized by Projekt DEAL.

Conflict of Interests

The authors declare no conflict of interest.

Data Availability Statement

The data that support the findings of this study are available in the supplementary material of this article.

Keywords: carbene homologues · conjugation · cyclic (alkyl)(amino)carbenes · *N*-heterocyclic carbenes · subvalent compounds

[1] a) C. Präsang, D. Scheschkewitz, *Chem. Soc. Rev.* **2016**, *45*, 900; b) V. Nesterov, N. C. Breit, S. Inoue, *Chem. Eur. J.* **2017**, *23*, 12014; c) A. Rammo, D. Scheschkewitz, *Chem. Eur. J.* **2018**, *24*, 6866; d) C. Weetman, *Chem. Eur. J.* **2021**, *27*, 1941; e) F. Hanusch, L. Groll, S. Inoue, *Chem. Sci.* **2021**, *12*, 2001; f) F. Dankert, C. Hering-Junghans, *Chem. Commun.* **2022**, *58*, 1242.

[2] a) W. P. Neumann, *Chem. Rev.* **1991**, *91*, 311; b) N. N. Zemlyanskii, I. V. Borisova, M. S. Nechaev, V. N. Khrustalev, V. V. Lunin, M. Y. Antipin, Y. A. Ustynyuk, *Russ. Chem. Bull. Int. Ed.* **2004**, *53*, 980; c) Y. Mizuhata, T. Sasamori, N. Tokitoh, *Chem. Rev.* **2009**, *109*, 3479; d) M. Asay, C. Jones, M. Driess, *Chem. Rev.* **2011**, *111*, 354; e) C. Shan, S. Yao, M. Driess, *Chem. Soc. Rev.* **2020**, *49*, 6733; f) J. A. Cabeza, P. García-Álvarez, C. J. Laglera-Gándara, *Eur. J. Inorg. Chem.* **2020**, *2020*, 784; g) N. Sen, S. Khan, *Chem. Asian J.* **2021**, *16*, 705; h) R. J. Somerville, J. Campos, *Eur. J. Inorg. Chem.* **2021**, *2021*, 3488; i) M. Ghosh, N. Sen, S. Khan, *ACS Omega* **2022**, *7*, 6449; j) T. Y. Lai, J. C. Fettinger, P. P. Power, *Organometallics* **2022**, *41*, 1590; k) P. M. Keil, A. Soyemi, K. Weisser, T. Szilvási, C. Limberg, T. J. Hadlington, *Angew. Chem.* **2023**, *62*, e202218141; *Angew. Chem. Int. Ed.* **2023**, *135*, e202218141.

[3] D. Bourissou, O. Guerret, F. P. Gabbaı, G. Bertrand, *Chem. Rev.* **2000**, *100*, 39.

[4] M. N. Hopkinson, C. Richter, M. Schedler, F. Glorius, *Nature* **2014**, *510*, 485.

[5] M. Soleilhavoup, G. Bertrand, *Acc. Chem. Res.* **2015**, *48*, 256.

[6] M. Melaimi, R. Jazzar, M. Soleilhavoup, G. Bertrand, *Angew. Chem.* **2017**, *129*, 10180; *Angew. Chem. Int. Ed.* **2017**, *56*, 10046.

[7] A. Doddi, M. Peters, M. Tamm, *Chem. Rev.* **2019**, *119*, 6994.

[8] P. Bellotti, M. Koy, N. Hopkinson, F. Glorius, *Nat. Chem. Rev.* **2021**, *5*, 711.

[9] S. Kumar Kushvaha, A. Mishra, H. W. Roesky, K. Chandra Mondal, *Chem. Asian J.* **2022**, *17*, e202101301.

[10] K. E. Wentz, A. Molino, S. L. Weisflog, A. Kaur, D. A. Dickie, D. J. D. Wilson, R. J. Gilliard, *Angew. Chem.* **2021**, *133*, 13175; *Angew. Chem. Int. Ed.* **2021**, *60*, 13065.

[11] E. Welz, J. Böhnke, R. D. Dewhurst, H. Braunschweig, B. Engels, *J. Am. Chem. Soc.* **2018**, *140*, 12580.

[12] O. Back, M. Henry-Ellinger, C. D. Martin, D. Martin, G. Bertrand, *Angew. Chem.* **2013**, *125*, 2675; *Angew. Chem. Int. Ed.* **2013**, *52*, 2939.

[13] a) K. C. Mondal, H. W. Roesky, B. Dittrich, N. Holzmann, M. Hermann, G. Frenking, A. Meents, *J. Am. Chem. Soc.* **2013**, *135*, 15990; b) C. Mohapatra, S. Kundu, A. N. Paesch, R. Herbst-Irmer, D. Stalke, D. M. Andrada, G. Frenking, H. W. Roesky, *J. Am. Chem. Soc.* **2016**, *138*, 10429; c) S. Kundu, P. P. Samuel, A. Luebben, D. M. Andrada, G. Frenking, B. Dittrich, H. W. Roesky, *Dalton Trans.* **2017**, *46*, 7947.

[14] Y. Wang, Y. Xie, P. Wei, R. B. King, H. F. Schaefer, P. V. R. Schleyer, G. H. Robinson, *Science* **2008**, *321*, 1069.

[15] R. S. Ghadwal, H. W. Roesky, S. Merkel, J. Henn, D. Stalke, *Angew. Chem.* **2009**, *121*, 5793; *Angew. Chem. Int. Ed.* **2009**, *48*, 5683.

[16] A. C. Filippou, O. Chernov, G. Schnakenburg, *Angew. Chem.* **2009**, *121*, 5797; *Angew. Chem. Int. Ed.* **2009**, *48*, 5687.

[17] K. C. Mondal, H. W. Roesky, M. C. Schwarzer, G. Frenking, I. Tkach, H. Wolf, D. Kratzert, R. Herbst-Irmer, B. Niepötter, D. Stalke, *Angew. Chem.* **2013**, *125*, 1845; *Angew. Chem. Int. Ed.* **2013**, *52*, 1801.

[18] Y. Li, Y.-C. Chan, Y. Li, I. Purushothaman, S. De, P. Parameswaran, C. W. So, *Inorg. Chem.* **2016**, *55*, 9091.

[19] S. Khan, H. W. Roesky, *Chem. Eur. J.* **2019**, *25*, 1636.

[20] A. J. Arduengo, H. V. R. Dias, J. C. Calabrese, F. A. Davidson, *Inorg. Chem.* **1993**, *32*, 1541.

[21] P. A. Rupar, M. C. Jennings, K. M. Baines, *Organometallics* **2008**, *27*, 5043.

[22] A. J. Ruddy, P. A. Rupar, K. J. Bladek, C. J. Allan, J. C. Avery, K. M. Baines, *Organometallics* **2010**, *29*, 1362.

[23] J. Baumgartner, C. Marschner, *Rev. Inorg. Chem.* **2013**, *34*, 119.

[24] G. Prabusankar, A. Sathyanarayana, P. Suresh, C. N. Babu, K. Srinivas, B. P. R. Metla, *Coord. Chem. Rev.* **2014**, *269*, 96.

[25] V. Nesterov, D. Reiter, P. Bag, P. Frisch, R. Holzner, A. Porzelt, S. Inoue, *Chem. Rev.* **2018**, *118*, 9678.

[26] J. Hlina, J. Baumgartner, C. Marschner, L. Albers, T. Müller, *Organometallics* **2013**, *32*, 3404.

[27] A. Jana, V. Huch, H. S. Rzepa, D. Scheschkewitz, *Angew. Chem.* **2015**, *127*, 291; *Angew. Chem. Int. Ed.* **2015**, *54*, 289.

[28] P. A. Rupar, M. C. Jennings, P. J. Ragogna, K. M. Baines, *Organometallics* **2007**, *26*, 4109.

[29] Y. Li, K. C. Mondal, H. W. Roesky, H. Zhu, P. Stollberg, R. Herbst-Irmer, D. Stalke, D. M. Andrada, *J. Am. Chem. Soc.* **2013**, *135*, 12422.

[30] C. Gendy, J. M. Rautinen, A. Mailman, H. M. Tuononen, *Chem. Eur. J.* **2021**, *27*, 14405.

[31] Y. Li, K. C. Mondal, J. Lübben, H. Zhu, B. Dittrich, I. Purushothaman, P. Parameswaran, H. W. Roesky, *Chem. Commun.* **2014**, *50*, 2986.

[32] P. B. Hitchcock, M. F. Lappert, A. J. Thorne, *J. Chem. Soc. Chem. Commun.* **1990**, *22*, 1587.

[33] H. Braunschweig, P. B. Hitchcock, M. F. Lappert, L. J.-M. Pierssens, *Angew. Chem.* **1994**, *106*, 1181; *Angew. Chem. Int. Ed. Engl.* **1994**, *33*, 1156.

[34] W. Wang, S. Inoue, S. Yao, M. Driess, *J. Am. Chem. Soc.* **2010**, *132*, 15890.

[35] S.-H. Zhang, C.-W. So, *Organometallics* **2011**, *30*, 2059.

[36] S. Krupski, J. V. Dickschat, A. Hepp, T. Pape, F. E. Hahn, *Organometallics* **2012**, *31*, 2078.

[37] W. Wang, S. Inoue, S. Enthaler, M. Driess, *Angew. Chem.* **2012**, *124*, 6271; *Angew. Chem. Int. Ed.* **2012**, *51*, 6167.

[38] W. Wang, S. Inoue, E. Irran, M. Driess, *Angew. Chem.* **2012**, *124*, 3751; *Angew. Chem. Int. Ed.* **2012**, *51*, 3691.

[39] J. V. Dickschat, D. Heitmann, T. Pape, F. E. Hahn, *J. Organomet. Chem.* **2013**, *744*, 160.

[40] R. K. Siwatch, D. Yadav, G. Mukherjee, G. Rajaraman, S. Nagendran, *Inorg. Chem.* **2013**, *52*, 13384.

[41] D. Gallego, S. Inoue, B. Blom, M. Driess, *Organometallics* **2014**, *33*, 6885.

[42] C. Cui, M. M. Olmstead, J. C. Fettinger, G. H. Spikes, P. P. Power, *J. Am. Chem. Soc.* **2005**, *127*, 17530.

[43] Y.-P. Zhou, S. Raoufmoghaddam, T. Szilvási, M. Driess, *Angew. Chem.* **2016**, *128*, 13060; *Angew. Chem. Int. Ed.* **2016**, *55*, 12868.

[44] S. Bestgen, N. H. Rees, J. M. Goicoechea, *Organometallics* **2018**, *37*, 4147.

[45] P. Garg, D. Dange, C. Jones, *Eur. J. Inorg. Chem.* **2020**, *2020*, 4037.

[46] P. Garg, D. Dange, C. Jones, *Dalton Trans.* **2021**, *50*, 9118.

[47] M. Dehmel, M. A. Wünsche, H. Görls, R. Kretschmer, *Eur. J. Inorg. Chem.* **2021**, *2021*, 4806.

[48] M.-P. Lücke, S. Yao, M. Driess, *Chem. Sci.* **2021**, *12*, 2909.

[49] S.-C. Huo, Y. Li, D.-X. Zhang, Q. Zhou, Y. Yang, H. W. Roesky, *Chem. Asian J.* **2022**, *17*, e202200141.

[50] Y. Xiong, S. Dong, S. Yao, C. Dai, J. Zhu, S. Kemper, M. Driess, *Angew. Chem.* **2022**, *134*, e202209250; *Angew. Chem. Int. Ed.* **2022**, *61*, e202209250.

[51] B. Gehrhus, P. B. Hitchcock, M. F. Lappert, *Z. Anorg. Allg. Chem.* **2005**, *631*, 1383.

[52] A. V. Zabula, F. E. Hahn, T. Pape, A. Hepp, *Organometallics* **2007**, *26*, 1972.

[53] F. E. Hahn, A. V. Zabula, T. Pape, A. Hepp, *Eur. J. Inorg. Chem.* **2007**, *2007*, 2405.

[54] F. E. Hahn, A. V. Zabula, T. Pape, A. Hepp, *Z. Anorg. Allg. Chem.* **2008**, *634*, 2397.

[55] F. E. Hahn, A. V. Zabuka, T. Pape, A. Hepp, R. Tonner, R. Haunschild, G. Frenking, *Chem. Eur. J.* **2008**, *14*, 10716.

[56] S. Yao, M. Brym, K. Merz, M. Driess, *Organometallics* **2008**, *27*, 3601.

[57] F. E. Hahn, A. V. Zabula, T. Pape, F. Hupka, *Z. Anorg. Allg. Chem.* **2009**, *635*, 1341.

[58] L. Klemmer, A.-L. Thömmes, M. Zimmer, V. Huch, B. Morgenstern, D. Scheschkewitz, *Nat. Chem.* **2020**, *13*, 373.

[59] H. Maeda, T. Suzuki, M. Segi, *Photochem. Photobiol. Sci.* **2018**, *17*, 781.

[60] A. Pöcheim, G. A. Özpınar, T. Müller, J. Baumgartner, C. Marschner, *Chem. Eur. J.* **2020**, *26*, 17252.

[61] D. Nieder, L. Klemmer, Y. Kaiser, V. Huch, D. Scheschkewitz, *Organometallics* **2018**, *37*, 632.

[62] L. Klemmer, Y. Kaiser, V. Huch, M. Zimmer, D. Scheschkewitz, *Chem. Eur. J.* **2019**, *25*, 12187.

[63] D. Nieder, C. B. Yildiz, A. Jana, M. Zimmer, V. Huch, D. Scheschkewitz, *Chem. Commun.* **2016**, *52*, 2799.

[64] D. Dhara, V. Huch, D. Scheschkewitz, A. Jana, *Inorganics* **2018**, *6*, 6.

[65] A. Jana, V. Huch, D. Scheschkewitz, *Angew. Chem.* **2013**, *125*, 12401; *Angew. Chem. Int. Ed.* **2013**, *52*, 12179.

[66] A. Jana, I. Omlor, V. Huch, H. S. Rzepa, D. Scheschkewitz, *Angew. Chem.* **2014**, *126*, 10112; *Angew. Chem. Int. Ed.* **2014**, *53*, 9953.

[67] D. Nieder, V. Huch, C. B. Yildiz, D. Scheschkewitz, *J. Am. Chem. Soc.* **2016**, *138*, 13996.

[68] R. C. Fischer, P. P. Power, *Chem. Rev.* **2010**, *110*, 3877.

[69] M. Haas, M. Leypold, D. Schnalzer, A. Torvisco, H. Stueger, *Organometallics* **2015**, *34*, 5291.

[70] I. Bejan, D. Scheschkewitz, *Angew. Chem.* **2007**, *119*, 5885; *Angew. Chem. Int. Ed.* **2007**, *46*, 5783.

[71] N. M. Obeid, L. Klemmer, D. Maus, M. Zimmer, J. Jeck, I. Bejan, A. J. P. White, V. Huch, G. Jung, D. Scheschkewitz, *Dalton Trans.* **2017**, *46*, 8839.

[72] A. Fukazawa, Y. Li, S. Yamaguchi, H. Tsuji, K. Tamao, *J. Am. Chem. Soc.* **2007**, *129*, 14164.

[73] L. Li, T. Matsuo, D. Hashizume, H. Fueno, K. Tanaka, K. Tamao, *J. Am. Chem. Soc.* **2015**, *137*, 15026.

[74] Y. Fu, M. Li, W. Shen, *Mol. Simul.* **2009**, *35*, 1279.

[75] B.-G. Kim, X. Ma, C. Chen, Y. Le, E. W. Coir, H. Hashemi, Y. Aso, P. F. Green, J. Kieffer, J. Kim, *Adv. Funct. Mater.* **2012**, *23*, 439.

[76] N. Yin, L. Wang, Y. Lin, J. Yi, L. Yan, J. Dou, H.-B. Yang, X. Zhao, C.-Q. Ma, *Beilstein J. Org. Chem.* **2016**, *12*, 1788.

[77] H. Cui, J. Zhang, C. Cui, *Organometallics* **2013**, *32*, 1.

[78] C. Müller, D. M. Andrada, I.-A. Bischoff, M. Zimmer, V. Huch, N. Steinbrück, A. Schäfer, *Organometallics* **2019**, *38*, 1052.

[79] F. Meiners, W. Saak, M. Weidenbruch, *Organometallics* **2000**, *19*, 2835.

[80] B. Pampuch, W. Saak, M. Weidenbruch, *J. Organomet. Chem.* **2006**, *691*, 3540.

[81] M. Lazraq, J. Escudié, C. Couret, J. Satgé, M. Draeger, R. Dammel, *Angew. Chem.* **1988**, *100*, 885; *Angew. Chem. Int. Ed. Engl.* **1988**, *27*, 828.

[82] N. Tokitoh, K. Kishikawa, R. Okazaki, *J. Chem. Soc. Chem. Commun.* **1995**, *1995*, 1425.

[83] A. F. Pozharskii, O. V. Ryabtsova, V. A. Ozeryanskii, A. V. Degtyarev, O. N. Kazheva, G. G. Alexandrov, O. A. Dyachenko, *J. Org. Chem.* **2003**, *68*, 10109.

[84] R. Gajda, A. Katrusiak, *Cryst. Growth Des.* **2008**, *8*, 211.

[85] A. K. Wolf, J. Glinnemann, L. Fink, E. Alig, M. Bolte, M. U. Schmidt, *Acta Crystallogr. Sect. B* **2010**, *66*, 229.

[86] J. Escudie, H. Ranaivonjatovo, *Adv. Organomet. Chem.* **1999**, *44*, 113.

[87] V. N. Khabashesku, S. E. Boganov, D. Antic, O. M. Nefedov, J. Michl, *Organometallics* **1996**, *15*, 4714.

[88] N. P. Toltl, W. J. Leigh, *J. Am. Chem. Soc.* **1998**, *120*, 1172.

[89] D. M. Chipman, Q. Sun, G. N. R. Tripathi, *J. Chem. Phys.* **1992**, *97*, 8073.

[90] Deposition Numbers 2236120 (**6**) and 2236118 (**7**) contain the supplementary crystallographic data for this paper. These data are provided free of charge by the joint Cambridge Crystallographic Data Centre and Fachinformationszentrum Karlsruhe Access Structures service.

[91] a) C. Müller, D. M. Andrada, I.-A. Bischoff, M. Zimmer, V. Huch, N. Steinbrück, A. Schäfer, *Organometallics* **2019**, *38*, 1052; b) C. M. Weinstein, G. P. Junor, D. R. Tolentino, R. Jazzar, M. Melaimi, G. Bertrand, *J. Am. Chem. Soc.* **2018**, *140*, 9255.

[92] N. Kuhn, T. Kratz, *Synthesis* **1993**, *1993*, 561.

[93] A. J. Arduengo, R. Krafczyk, R. Schmutzler, H. A. Craig, J. R. Goerlich, W. J. Marshall, M. Unverzagt, *Tetrahedron* **1999**, *55*, 14523.

[94] G. R. Fulmer, A. J. M. Miller, N. H. Sherden, H. E. Gottlieb, A. Nudelman, B. M. Stoltz, J. E. Bercaw, K. I. Goldberg, *Organometallics* **2010**, *29*, 2176.

[95] G. M. Sheldrick, *Acta Crystallogr. Sect. A* **2015**, *71*, 3.

[96] G. M. Sheldrick, *Acta Crystallogr. Sect. C* **2015**, *71*, 3.

[97] C. B. Hübschle, G. M. Sheldrick, B. Dittrich, *J. Appl. Crystallogr.* **2011**, *44*, 1281.

[98] Gaussian 09, Revision A.02, M. J. Frisch, G. W. Trucks, H. B. Schlegel, G. E. Scuseria, M. A. Robb, J. R. Cheeseman, G. Scalmani, V. Barone, G. A. Petersson, H. Nakatsuji, X. Li, M. Caricato, A. Marenich, J. Bloino, B. G. Janesko, R. Gomperts, B. Mennucci, H. P. Hratchian, J. V. Ortiz, A. F. Izmaylov, J. L. Sonnenberg, D. Williams-Young, F. Ding, F. Lipparini, F. Egidi, J. Goings, B. Peng, A. Petrone, T. Henderson, D. Ranasinghe, V. G. Zakrzewski, J. Gao, N. Rega, G. Zheng, W. Liang, M. Hada, M. Ehara, K. Toyota, R. Fukuda, J. Hasegawa, M. Ishida, T. Nakajima, Y. Honda, O. Kitao, H. Nakai, T. Vreven, K. Throssell, J. A. Montgomery, Jr., J. E. Peralta, F. Ogliaro, M. Bearpark, J. J. Heyd, E. Brothers, K. N. Kudin, V. N. Staroverov, T. Keith, R. Kobayashi, J. Normand, K. Raghavachari, A. Rendell, J. C. Burant, S. S. Iyengar, J. Tomasi, M. Cossi, J. M. Millam, M. Klene, C. Adamo, R. Cammi, J. W. Ochterski, R. L. Martin, K. Morokuma, O. Farkas, J. B. Foresman, D. J. Fox, Gaussian, Inc., Wallingford CT, **2016**.

[99] a) J. P. Perdew, *Phys. Rev. B* **1986**, *33*, 8822; b) A. D. Becke, *Phys. Rev. A* **1988**, *38*, 3098.

[100] a) A. Schäfer, H. Horn, R. Ahlrichs, *J. Chem. Phys.* **1992**, *97*, 2571; b) A. Schäfer, C. Huber, R. Ahlrichs, *J. Chem. Phys.* **1994**, *100*, 5829; c) F. Weigend, R. Ahlrichs, *Phys. Chem. Chem. Phys.* **2005**, *7*, 3297; d) F. Weigend, *Phys. Chem. Chem. Phys.* **2006**, *8*, 1057.

[101] S. Grimme, J. Antony, S. Ehrlich, H. Krieg, *J. Chem. Phys.* **2010**, *132*, 154104.

[102] NBO 7.0. E. D. Glendening, J. K. Badenhoop, A. E. Reed, J. E. Carpenter, J. A. Bohmann, C. M. Morales, P. Karafiloglou, C. R. Landis, F. Weinhold, Theoretical Chemistry Institute, University of Wisconsin, Madison **2018**.

[103] F. Neese, F. Wennmohs, U. Becker, C. Riplinger, *J. Chem. Phys.* **2020**, *152*, 224108.

[104] a) J. P. Perdew, M. Ernzerhof, K. Burke, *J. Chem. Phys.* **1996**, *105*, 9982; b) C. Adamo, V. Barone, *J. Chem. Phys.* **1999**, *110*, 6158.

[105] Chemcraft – graphical software for visualization of quantum chemistry computations. http://www.chemcraftprog.com.

Manuscript received: April 21, 2023
Accepted manuscript online: April 28, 2023
Version of record online: May 19, 2023